Mechanical weakness of thoracic aorta related to aging or dissection predicted by speed-of-sound with collagenase

Mechanical weakness of thoracic aorta related to aging or dissection predicted by speed-of-sound with collagenase

Katsutoshi Miura[a,*] and Kanna Yamashita[a]

[a]Department of Health Science, Pathology and Anatomy, Hamamatsu University School of Medicine, Hamamatsu, Japan

*Corresponding author

1-20-1 Handa-yama, Higashiku, Hamamatsu 431-3192, Japan

Tel: 81-53-435-2811

Fax: 81-53-435-2800

E-mail: kmiura@hama-med.ac.jp

Abstract

Scanning acoustic microscopy reveals information about histology and speed-of-sound (SOS) through tissues. Slower SOS corresponds to lower stiffness. The present study aimed to investigate whether SOS values reflect the degree of degeneration with aging or dissection and whether enzymatic digestion susceptibility is distinct. SOS of media besides the atheromatous areas of normal and surgical dissections was measured and compared using medial degeneration grade (MDG) scores. To evaluate the damage rate, SOS was assessed following collagenase digestion. SOS scores negatively correlated with aging and MDG scores. Dissected aortae showed higher SOS and MDG scores without age correlation. Collagenase digestion was present in all aortae, but older aortae were more injured than younger aortae. Dissected aortae were more vulnerable to collagenase. Older and dissected aortae expressed specific extracellular matrix (ECM) components to compensate for mechanical weakness. The present method can evaluate mechanical weakness corresponding to histology to investigate the cause of rupture.

Keywords: scanning acoustic microscopy, collagenase, extracellular matrix, thoracic aorta, medial degeneration grade, aging, dissected aorta

Introduction

Aortic diseases are a major health concern that may result in aneurysm, dissection, and atherosclerotic occlusion (Tsamis et al. 2013). A normally elastic aorta can begin to stiffen with age (Radu-Ionita et al. 2017). Losing elasticity due to conditions such as atherosclerosis or Marfan (MF) syndrome causes serious disorders.

The aortic wall media are organized into lamellar units, comprising concentric layers of elastic lamellae, smooth muscle cells, and interlamellar matrix (Brooke et al. 2003). Elastic fibers are predominantly composed of elastin, whereas the interlamellar matrix contains structural/supporting proteins, such as type-I collagen, type-III collagen, and fibrillin (FBN). All extracellular matrix (ECM) components provide structural organization and stability to the vessel wall through interactions between the smooth muscle cells and associated ECM elements. Moreover, these elements include lysyl oxidase (LOX), vitronectin (VN), and fibronectin (FN). Collagens bind and signal to smooth muscle cells through specific matrix receptors. Elastic fibers are linked to smooth muscle cells through a microfibril scaffold consisting of FBN and microfibril-associated glycoproteins.

All aortic diseases are associated with microstructural changes in the content or architecture of the connective fibers (Tsamis et al. 2013). Connective fibers consist of

elastin and collagen (Tsamis et al. 2013), which confer elasticity and strength to a healthy aorta, respectively. Matrix metalloproteinases (MMPs), which include collagenases, are a family of endopeptidases with proteolytic activity toward both elastin and collagen (Choke et al. 2005). The high collagenase activity of the aorta contributes to aneurysms and rupture (Menashi et al. 1987; Busuttil 1980). MMP-1 (collagenase-1), -8 (collagenase 2), and -13 (collagenase-3) are enzymes specific for collagens. Collagenase-3 was used to imitate biochemical injury to aortae and detect susceptibility to aneurysm and aortic rupture.

The elasticity of the aortae has been reported in dogs (Hughes et al. 1979) and humans (Sutton-Tyrrell et al. 2005; Lehmann et al. 1993) by measuring pulsed wave velocity. Other methods to estimate aortic elasticity *in vivo* include elastography (Fromageau et al. 2008) or micro-elastography (Schmitt et al. 2010), which use shear waves, and 4D ultrasound (Wittek et al. 2013) which apply time-resolved three dimensional ultrasound.

These methods can provide macroscopic information about the elasticity of the entire arterial wall, including the intima, media, and adventitia. However, they do not address local tissue elements such as smooth muscle loss, accumulation of ECM components, aneurysm, and dissection.

Scanning acoustic microscopy (SAM) can evaluate both histological and viscoelastic properties (Mamou and Rohrbach 2017; Miura 2016; Saijo 2009). Since Lemons and Quate (1974) at Stanford University provided the basic design of SAM in the biomedical field, many studies have reported on biological objects at low frequencies (ranging from 1 to 10 MHz) (Maev 2008). Studies of the acoustic properties of tissues at low frequencies suggest that SOS in soft tissues differs only slightly from its value in water and is virtually independent of frequency (Duck 1990). Only solid tissue, such as bones, and tissues rich in fibrillar proteins showed significant differences. Many acoustic images were collected and analyzed by Quate's team, primarily using fixed unstained tissues. Low-frequency studies (1 to 7 MHz) of acoustic parameters of tissues (attenuation coefficients, SOS) have demonstrated that fixation in 4% formalin changes these parameters only slightly (Bamber et al. 1979).

Studies of acoustic properties of biological tissues at high frequencies (> 100 MHz) have recently began to obtain high-resolution quantitative images. Improvements such as transducers with a very small F-number and high sensitivity (Mamou and Rohrbach 2017) and time-frequency analysis method (Hozumi et al. 2004) have contributed to this progress. Even single cells can now be

identified in the subcellular structures (Lemor et al. 2004; Weiss et al. 2007) and clinical cytology samples (Miura and Yamamoto 2015).

The speed-of-sound (SOS) of tissues observed using SAM is given as:

$$\boldsymbol{c = \sqrt{K/\rho}},$$

where c is the SOS, K is the elastic bulk modulus, and ρ is the density.

This formula implies that the SOS strongly reflects its elastic parameter. SOS values (m/sec)have been reported for many tissues (Azhari 2010; Saijo et al. 1998)**.** In general, SOS has low values in fluid-filled soft structures and high values in dense solid tissues. SOS values are well-correlated with the palpable tissue stiffness. Therefore, ultrasound, *in vivo* imaging-based methods such as elastography (Mahmood et al. 2016), and *in vitro* tests on isolated samples, such as the SAM method, are available for estimating the mechanical properties of biological samples. The current study used a stored collection of ascending aorta (AAo) surgical specimens with detailed clinical history, including dissection episode, to investigate the elasticity of the specimen and observe histology to gain etiological insights.

Aortic walls progressively lose their components and increase their content in fibrous tissue, leading to greater stiffness with aging. Aging aortae can lead to two

conditions involving greater or thinner wall thickness (Tsamis et al. 2013). The first is atherosclerosis, which causes wall thickening due to development of a fatty plaque. The second is aneurysm, which is produced by balloon-like thinning of the wall due to local weakness. Focal portions of aortae fail to compensate mechanical strength to form aneurysm or second bleb in aneurysm. The specific etiology of dissection due to aging or genetic defects is unknown to date (Wu et al. 2013).

The aim of the present study was to investigate whether SOS values reflect the degree of aortic degeneration and whether resistance to collagenase digestion is different between aged and dissected cases. Moreover, the biochemical changes in ECM components were compared between aging aortae and dissected aortae.

Materials and Methods

Subjects and ethics

All human tissue sections were obtained from samples stored in the tissue archives of the Hamamatsu University Hospital or Shizuoka City Hospital in Japan. The AAo of adult autopsied patients without serious cardiovascular diseases were consecutively selected to investigate the effects of aging on the biomechanical properties of the aortae (n = 36; age, 62.9 ± 20.0 years; 24 men and 12 women). Cases of MF syndrome (n = 7;

age, 46.7 ± 16.2 years; three men and four women) and non-MF syndrome (n = 9; age, 56.3 ± 12.0 years; seven men and two women) were selected from surgical specimens of dissected AAo aneurysm with known clinical history. Formalin-fixed, paraffin-embedded (FFPE) tissue blocks were flat-sectioned into 10-μm-thick slices and observed using SAM. The research protocol for using stored samples without a link to patient identity was approved by the Ethics Committee of Hamamatsu University School of Medicine (No. 14-135, 19-180). Written consent was waived based on the retrospective design. All procedures were conducted according to approved guidelines and regulations.

SAM observations

The experimental protocol is detailed in Fig. 1. Aortic tissue specimens were evaluated using SAM system (AMS-50AI, Honda Electronics, Toyohashi, Aichi, Japan) with a central frequency of 320 MHz, lateral resolution of 3.8 μm, and thickness of the focal spot of 13 μm. A single-pulsed ultrasound with 2-ns pulse width was emitted (Hozumi et al. 2004). Distilled water was used for coupling fluid between the transducer and the specimen. The transducer was used for both transmitting and receiving the signal. Reflected waveforms from the surface and

the bottom of specimen were compared to measure the SOS and the thickness of each point. Waveform from the glass surface without the specimen present was used as a reference waveform.

Scanning the transducer over the specimen formed an acoustic image. The mechanical scanner was arranged so that the ultrasonic beam was transmitted at every 8, 4 and 2 μm interval over a 2.4, 1.2, and 0.6 mm width, respectively. The number of sampling points was 300 in one scanning line, and 300 x 300 points made one frame. Four pulse echo sequences were arranged for each scan point in order to increase the signal-to-noise-ratio. Each pixel of an image corresponds to an echo coming from an x-y position on the specimen.

The observed samples were prepared by cutting FFPE blocks. Although FFPE samples have been demonstrated as having slightly higher SOS than fresh samples, the SOS values were stable (Sasaki et al. 1996) irrespective of periods of formalin fixation from 1 day to 3 months (Miura et al. 2015). Therefore, sample bias due to fixation condition was negligible. Areas without calcified deposits and heavy atheroma were selected for comparison. **Calcified areas result in chatter marks on the section, which causes irregular reflection and heavy atheromatous portions become translucent due to lipid dissolution in organic solvents. In dissected cases, non-dissected portions**

away from the separation were used for SOS measurement.

SOS difference according to age and disease status (normal, MF syndrome, and non-MF syndrome)

To evaluate age-related changes of the aorta, the average SOS values of the aortic media were plotted according to age. To compare the mechanical weakness and structural differences, the samples were divided into two groups: (1) younger adults aged 31–58 years (average, 46.7 ± 11.47 years; n = 6; four men and two women) and (2) older individuals aged 76−85 years (average, 80.2 ± 3.42 years; n = 5; four men and one woman). The SOS values of dissected aortae (including MF syndrome and non-MF syndrome) (n = 16; age 52.1 ± 14.3 years; 10 men and 6 women) were also compared with age-matched normal aortae (n = 12; age 56.8 ± 15.7 years; 8 men and 4 women) by plotting the average SOS values of the aortic media according to age.

Catalytic damage according to collagenase digestion

Paraffin sections were dewaxed using xylene, soaked in distilled water, and submerged into a solution of phosphate-buffered saline containing 0.5 mM $CaCl_2$ (pH 7.4) plus 250 units/mL type-III collagenase (Worthington, Lakewood, NJ, USA) at 37°C for 1.5 h or

176 twice for 1.5 h (Miura and Katoh 2016). According to the manufacturer's instructions,
177 type-III collagenase has typical collagenase activity but lower proteolytic activity than
178 other collagenases. SOS was measured both before (baseline) and after digestion.
179 Digested sections were first washed with distilled water before being analyzed with
180 SAM. The same sections were measured after a repeated digestion (two 1.5-h
181 treatments).
182
183 ***Medial degeneration grade (MDG) evaluation***
184 To compare SAM with light microscopy (LM) images, the same or nearby sections were
185 stained with hematoxylin, eosin, and Elastica Masson trichrome (EMT) to stain collagen
186 and elastic fibers blue and black, respectively. The magnification of each LM image was
187 adjusted to match the corresponding SAM image with scale bars on the bottom and the
188 left side of the screen frame.
189 Consensus criteria was used to evaluate the extent and severity of the aortic
190 MDG scores (Halushka et al. 2016). These criteria included mucoid extracellular matrix
191 accumulation, elastic fiber fragmentation/loss, smooth muscle cell nuclei loss, and
192 laminar medial collapse. The overall MDG was scored as 0 (none), 1 (mild), 2
193 (moderate), or 3 (severe).

194

195 ***Immunohistochemical analysis***

196 Immunostaining was performed using a commercially available Chemmate envision kit
197 (Dako, Glostrup, Denmark). The following primary antibodies used: anti-smooth
198 muscle actin (SMA) (ab5694, Abcam, Tokyo, Japan; 1:400), anti-collagen I (ab88147,
199 Abcam, 1:100) and anti-collagen III (ab7778, Abcam, 1:1000) for collagen types,
200 anti-LOX (ab174316, Abcam, 1:300), anti-VN (ab46808, Abcam, 1:250), anti-FBN
201 (ab53076, Abcam, 1:25), and anti-FN (ab2413, Abcam, 1:250). Heat-mediated antigen
202 (95°C, 20 min) was retrieved with buffer balanced to either pH 6.0 (anti-SMA,
203 anti-collagen III, FN) or pH 9.0 (anti-collagen I, anti-LOX, anti-VN) before staining.

204

205 ***Statistical analyses***

206 The average SOS values of the aortic media were calculated from at least five images
207 per case using the SAM manufacturer and commercial statistics software
208 (Statcel3-Addin forms on Excel, OMS publishing, Tokorozawa, Saitama, Japan), which
209 calculates the average areas-of-interest values. To detect the correlations between age
210 and SOS values and between age and MDG scores, scatter plots were established and
211 subjected to simple linear regression analysis. The correlation strength was quantified

using Pearson's correlation coefficients (r). The average SOS (± SD) values from younger and older aortae and between dissected aortae and age-matched normal aortae were compared using unpaired Student's t-tests. The average SOS values (± SD) among different time points after collagenase were compared using paired t-tests.

It was confirmed that each data set followed a normal distribution pattern before statistical analyses were conducted. Significance level for all tests was set at $p < 0.05$.

Results

Age-dependent changes in SOS and MDG of normal aortic media

SOS values of the normal aortic media without calcified deposits and heavy atheroma potions decreased with age (Fig. 2a). SOS values were negatively correlated with age ($y = -0.6032x + 1699.3$, $r = -0.39$, $p = 0.015$).

The significantly positive relationship between age and MDG scores ($y = 0.021x + 0.21$, $r = 0.56$, $p = 0.0003$) is shown in Figure 2b. **The significantly negative relationship between SOS and MDG scores ($y = -0.012x + 22.47$, $r = -0.505$, $p = 0.0016$) is shown in Figure 2c.**

Relationship between age and SOS or MDG of dissected aortae

SOS values and MDG scores of dissected aortae were compared with those of age-matched normal ones (Fig. 2d). The dissection group exhibited significantly greater SOS values (p = 8.50E-10) and higher MDG scores (p = 0.043) than the normal group. No significant correlation between age and SOS values ($y = -0.2334x + 1738$, $r = -0.17$, $p = 0.501$) (Fig. 2a) or age and MDG scores ($y = 0.0025x + 1.83$, $r = 0.075$, $p = 0.772$) (Fig. 2b) was observed in dissected aortae. **There was also no significant relationship between SOS value and MDG scores ($y = -0.0054x + 11.45$, $r = -0.21$, $p = 0.42$) (Fig. 2c).**

Differential changes in SOS values between older and younger aortae after collagenase digestion

Before collagenase digestion, the older aortic media (n = 22) showed significantly lower SOS values than the younger aortae (n = 20) (Figs. 3a and 3b; Table A1). After collagenase digestion, both older and younger aortae showed lower SOS values. At 1.5 h after digestion, SOS values significantly decreased in both cases ($p < 0.01$) (Fig. 4). EMT staining revealed wavy, thin, and split elastic fibers in the media from the older aorta, whereas the younger aortae contained thicker and straighter fibers. LM images obtained 3 h after digestion revealed numerous fragmented elastic fibers in the older

aortae compared to the younger aortae. Similar to the baseline difference at 0 h, older aortae had significantly lower SOS values than younger aortae after 1.5 h and 3 h of collagenase digestion (p's < 0.01).

Differential changes in SOS values between dissected aortae (MF and non-MF syndrome) and normal aortae after collagenase digestion

Cases of dissected aortae with MF had cystic mucoid degeneration and elastic fiber fragmentation or loss. Cystic degeneration displayed low SOS values (Fig. 3c). Non-MF cases consisting of thick parallel muscles and wavy elastic fibers with focal splitting showed high SOS values (Fig. 3d). SOS values decreased faster after digestion in cases of dissected aortae compared to age-matched controls (Fig. 4 and Table A2). At baseline, the two groups showed significantly different SOS values (p = 0.0001). However, the difference in SOS values disappeared after 1.5 h (p = 0.100) and 3 h (p = 0.346). In contrast to the SOS results, LM images in EMT staining showed no major differences between MF syndrome and non-MF syndrome cases. There was slight muscle fiber disappearance and loose elastic fibers before and after digestion.

Structure components of SMA, collagen type-I, and collagen type-III in the older,

younger, MF, and non-MF aortae

Regarding SMA immunostaining (Fig. 5a), old aortae showed focal loss of smooth muscles, whereas younger aortae consisted of continuous parallel muscles. MF cases displayed aggregated muscle fibers with irregular arrangement, whereas non-MF cases showed scattered loss of smooth muscle fibers.

Regarding collagen type-I (Fig. 5b) and type-III (Fig. 5c), normal young and old cases displayed parallel collagen fibers. Non-MF cases had rich collagen fibers, although fiber arrangement was irregular. MF cases had poor collagen fibers with irregular arrangement among cells. Table 1 details the immunohistochemical results.

ECM components of LOX, VN, FBN, and FN in the younger, older, MF, and non-MF aortae

Immunostaining with anti-LOX (Fig. 6a) showed that normal younger and older aortae exhibited no to faint positive staining. However, the MF aortae revealed strong punctate-patterned staining on smooth muscles, whereas the non-MF aortae showed weak positive staining.

Regarding the VN (Fig. 6b), all normal young or old aortae and MF and non-MF ones were focally positive, although MF cases showed a rather irregular

distribution.

About FBN (Fig. 6c), all cases except MF were positive. Concerning FN (Fig. 6d), old and non-MF cases were positively associated with muscle fibers, whereas young and MF aortae exhibited negative or focal weak positivity.

Discussion

Both structural and mechanical alterations in AAo were found with aging and dissection cases using SAM combined with collagenase treatment and immunostaining. Age was negatively correlated with SOS values based on SAM results, suggesting that the non-atheromatous or calcified portions of the aorta become mechanically weaker with age. In general, aging aortic walls show an increased stiffness due to atherosclerosis and calcification. However, non-atheromatous portions of media showed loose and irregular arrangement of smooth muscles and collagen fibers, which contributed to aneurysms and rupture. **The MDG scores that increased with aging were significantly negatively correlated with SOS values of non-atheromatous portions. The dissected aortae cases, in which SOS values and MDG scores were both higher than those of their age-matched controls, showed no significant alteration with aging.** This may

302 indicate that dissected aortic walls have greater stiffness to compensate for structural
303 defects, but are focally fragile and prone to ruptures. The susceptibility to collagenase
304 digestion supported this speculation. Other risk factors for dissection apart from aging
305 must also be present, such as genetic susceptibility. Not only MF syndrome cases but
306 also non-MF young cases may present genetic defects of ECM components.
307 Regarding damage caused by collagenases, both young and older cases
308 exhibited significantly decreased SOS values following 1.5 h and 3 h of collagenase
309 treatment. Young aortae retained rather high SOS values even after 3 h, whereas older
310 aortae reached minimum values close to the risk threshold of rupture. At 3 h, the old
311 aortae were composed of loose filamentous fibers. The dissected aortae group, including
312 MF and non-MF cases, had very high SOS values at baseline and more rapidly
313 decreased values after 1.5 h and 3 h as compared to their age-matched controls.
314 **Dissected aortae may have greater stiffness due to compensation for structural**
315 **defects. Sufficient number of structural components offset fragile quality, as seen**
316 **in smooth muscle bundles of MF cases and rich collagen type-III fibers of non-MF**
317 **cases.**
318 The fibrous portions of the dissected aortae had consistent SOS values,
319 whereas the non-fibrous portions were more sensitive to enzymatic damages. Busuttil et

al. (1980) reported that collagenase activity is detected in the aneurysmal wall of abdominal aorta. Therefore, positive results for collagenase testing may predict future rupture.

Immunostaining of the structural fibers in young aortae showed a continuous parallel array, while the structural fibers in the old aortae were divided or sparse. Regarding ECM proteins, FN was enriched in the older aortae compared to the younger aortae. In the dissected aortae, MF cases had irregular distribution of SMA, collagen I, and collagen III fibers, whereas most non-MF cases had distribution that was similar to the normal older aortae. MF cases were positive for LOX and VN antigens, although FBN and FN immunostaining was negative or faint. Both non-MF and elderly cases exhibited a similar pattern of positivity for LOX, VN, FBN, and FN.

The histopathological alterations in dissection cases include smooth muscle cell disappearance, medial mucoid degeneration, and ECM breakdown (Michel et al. 2018; Wu et al. 2013). Dissection is performed because of genetic causes or degeneration with aging (Michel et al. 2018). Among the 29 thoracic dissected aortae-associated genes identified to date, the majority encode proteins involved in the extracellular matrix, smooth muscle cell contraction or metabolism, or transformation of the growth factor-β signaling pathway (Brownstein et al. 2017). SMA, collagens 1 and 3, elastin, FBN1, and

LOX are also included. MF syndrome, an autosomal dominant inherited disorder caused by mutations in FBN1 (Dietz 1991), was reported to have increased expression of matrix metalloproteinase (MMP)-2 and MMP-9 and premature aortic smooth muscle cell differentiation (Dale et al. 2017).

Regarding ECM proteins, LOX is an extracellular amine oxidase that primarily functions as a catalyst on the covalent cross-linking of collagen and elastin fibers in ECM (Kagan and Li 2003). VN in ECM is involved in tissue repair and remodeling (Leavesley et al. 2013). FBN-1 plays a crucial role in stabilizing the structure of elastic fiber. FN plays roles in cell adhesion, migration, growth, and differentiation (Sottile 2002). FN in ECM controls deposition, organization, and stability of other matrix proteins, including type-I collagen and type-III collagen. Specific types of ECM proteins are expressed differently among MF, non-MF, and normal old cases to maintain the mechanical strength of the aortic wall.

Although the resolution and flexibility in SAM imaging is not better than LM imaging, it still has several advantages. First, no staining is required, which allows for imaging of the sample within a few minutes. **Second, SOS values are digital, allowing easy quantitative comparison among lesions.** Third, the virtual color images of SOS values are adjustable based on the range of interest, facilitating easy detection of

abnormal regional alterations. Fourth, protease digestion alterations can be repeatedly monitored with greater sensitivity compared to LM.

This study has several limitations that should be acknowledged. First, the observed tissues were FFPE sections. Compared with fresh tissues, tissues fixed for extended periods, such as those used for autopsies, become harder. However, the current study reported SOS values in normal autopsy cases that were lower than those in surgical specimens. The SOS values of fresh and formalin-fixed aortae have been previously reported. Akhtar et al. (2016) reported that the SOS value of fresh aortae was between 1,538 and 1,709 m/s. Saijo et al. (1998) reported SOS values of 1,614 ± 30 m/s in formalin-fixed frozen sections of the aorta without paraffin-embedded treatment. Our cases showed that the overall **mean** SOS value was 1,648.4 ± 30.2 m/s (age range, 16–101 years), indicating that SOS values in the FFPE aortae were somewhat greater than those in fresh-frozen aortae, but similar to those previously reported. Sasaki et al. (1996) reported the influence of formalin fixation on the acoustic properties of the normal kidney. No significant differences in acoustic parameters, including SOS values or attenuation were observed. The second limitation is that sex differences were not considered. The consecutive autopsy and surgical tissue samples used were predominantly from men, with a few samples from younger women. Because fewer

374 younger and postmenopausal women present with similar vascular alterations as men
375 (Waddell et al. 2001), gender bias may be low. Third, the non-MF group included
376 different etiologies; therefore, LM images might be distinctly different in non-MF cases.
377 However, these non-MF cases had some common histological findings, such as an
378 intralamellar mucoid matrix and fragmentation or thinning of the elastic fibers, as
379 demonstrated in representative images. Despite these limitations, SAM analysis with
380 protease digestion is a useful method to evaluate mechanical weakness due to histology
381 features and to investigate the cause of rupture.

382 **In conclusion, SOS values appropriately reflected mechanical weakness**
383 **and degeneration with aging. Dissected aortae had higher SOS values irrespective**
384 **of high MDG scores. All normal and dissected aortae were vulnerable to**
385 **collagenase digestion. Old aortae first reached the lowest level of SOS, and**
386 **compared with normal aortae, dissected ones showed more susceptible to**
387 **collagenase digestion. Old and dissected aortae had different structural**
388 **components to protect against mechanical weakness of the thoracic aorta.**

389

390

Acknowledgments

The authors thank T. Moriki, Y. Egawa, Y. Kawabata, and N. Suzuki for their help in preparing the histological samples, Dr K. Kobayashi for his technical supports and advices with SAM, and to Enago (www.enago.jp) for the English language review.

Funding

This work was supported by a grant from the Japan Society for the Promotion of Science (KAKENHI), Scientific Research Grant Number (c) 15K08375.

Conflict of interest

None.

403 **References**

404 Akhtar R, Cruickshank JK, Zhao X, Derby B, Weber T. A pilot study of scanning
405 acoustic microscopy as a tool for measuring arterial stiffness in aortic biopsies.
406 Artery Res Elsevier Ltd 2016;13:1-5.

407 Azhari H. Appendix A: Typical Acoustic Properties of Tissues. Basics Biomed
408 Ultrasound Eng Wiley-IEEE Press 2010:pp. 313-314.

409 Bamber JC, Hill CR, King JA, Dunn F. Ultrasonic propagation through fixed and
410 unfixed tissues. Ultrasound Med Biol 1979;5:159-165.

411 Brooke BS, Karnik SK, Li DY. Extracellular matrix in vascular morphogenesis and
412 disease: structure versus signal. Trends Cell Biol Elsevier Current Trends
413 2003;13:51-56.

414 Brownstein AJ, Ziganshin BA, Kuivaniemi H, Body SC, Bale AE, Elefteriades JA.
415 Genes associated with thoracic aortic aneurysm and dissection-an update and
416 clinical implications. Aorta 2017;5:11-20.

417 Busuttil RW. Collagenase activity of the human aorta. Arch Surg 980;115:1373-1378.

418 Choke E, Cockerill G, Wilson WRW, Sayed S, Dawson J, Loftus I, Thompson MM. A
419 review of biological factors implicated in abdominal aortic aneurysm rupture. Eur.
420 J Vasc Endovasc Surg 2005;30:227-44.

421 Dale M, Fitzgerald MP, Liu Z, Meisinger T, Karpisek A, Purcell LN, Carson JS,
422 Harding P, Lang H, Koutakis P, Batra R, Mietus CJ, Casale G, Pipinos I, Baxter
423 BT, Xiong W. Premature aortic smooth muscle cell differentiation contributes to
424 matrix dysregulation in Marfan Syndrome. PLoS One 2017;12:1-18.
425 Dietz H et al. Marfan syndrome caused by a recurrent de novo missense mutation in the
426 fibrillin gene. Nature 1991;352:337-9.
427 Duck FA. Acoustic properties of tissue at ultrasonic frequencies. In: Duck FA, ed. Phys
428 Prop Tissues London: Academic Press, 1990. pp. 73-135.
429 Fromageau J, Lerouge S, Maurice RL, Soulez G, Cloutier G. Noninvasive vascular
430 ultrasound elastography applied to the characterization of experimental aneurysms
431 and follow-up after endovascular repair. Phys Med Biol 2008;53:6475-6490.
432 Halushka MK, Angelini A, Bartoloni G, Basso C, Batoroeva L, Bruneval P, Buja LM,
433 Butany J, d'Amati G, Fallon JT, Gallagher PJ, Gittenberger-de Groot AC, Gouveia
434 RH, Kholova I, Kelly KL, Leone O, Litovsky SH, Maleszewski JJ, Miller D V,
435 Mitchell RN, Preston SD, Pucci A, Radio SJ, Rodriguez ER, Sheppard MN, Stone
436 JR, Suvarna SK, Tan CD, Thiene G, Veinot JP, van der Wal AC. Consensus
437 statement on surgical pathology of the aorta from the Society for Cardiovascular
438 Pathology and the Association For European Cardiovascular Pathology: II.

439 Noninflammatory degenerative diseases - nomenclature and diagnostic criteria.
440 Cardiovasc Pathol 2016;25:247-257.
441 Hozumi N, Yamashita R, Lee CK, Nagao M, Kobayashi K, Saijo Y, Tanaka M, Tanaka
442 N, Ohtsuki S. Time-frequency analysis for pulse driven ultrasonic microscopy for
443 biological tissue characterization. Ultrasonics 2004. pp. 717-722.
444 Hughes DJ, Babbs CF, Geddes LA, Bourland JD. Measurements of Young's modulus
445 of elasticity of the canine aorta with ultrasound. Ultrason Imaging 1979;1:356-367.
446 Kagan HM, Li W. Lysyl oxidase: Properties, specificity, and biological roles inside and
447 outside of the cell. J Cell Biochem 2003;88:660-72
448 Leavesley DI, Kashyap AS, Croll T, Sivaramakrishnan M, Shokoohmand A, Hollier BG,
449 Upton Z. Vitronectin - Master controller or micromanager? IUBMB Life
450 2013;65:807-818.
451 Lehmann ED, Parker JR, Hopkins KD, Taylor MG, Gosling RG. Validation and
452 reproducibility of pressure-corrected aortic distensibility measurements using
453 pulse-wave-velocity Doppler ultrasound. J Biomed Eng 1993;15:221-228.
454 Lemons RA, Quate CF. Acoustic microscope - Scanning version. Appl Phys Lett
455 1974;24(4):163-5.
456 Lemor RM, Weiss EC, Pilarczyk G, Zinin P V. Mechanical properties of single cells:

457 Measurement possibilities using time-resolved scanning acoustic microscopy. Proc
458 - IEEE Ultrason Symp 2004.
459 Maev RG. Acoustic properties of biological tissues and their effect on the image
460 contrast. Acoust Microsc Weinheim, Germany: Wiley-VCH, 2008. pp. 212-231.
461 Mahmood B, Ewertsen C, Carlsen J, Nielsen M. Ultrasound vascular elastography as a
462 tool for assessing atherosclerotic plaques - A systematic literature review.
463 Ultrasound Int Open 2016;02:E106-E112.
464 Mamou J, Rohrbach D. Image formation methods in quantitative acoustic microscopy
465 Jonathan Mamou and Daniel Rohrbach F . L . Lizzi Center for Biomedical
466 Engineering Riverside Research New York , NY , USA. IEEE Int Conf Acoust
467 Speech, Signal Process 2017;6259-6263.
468 Menashi S, Campa JS, Greenhalgh RM, Powell JT. Collagen in abdominal aortic
469 aneurysm: Typing, content, and degradation. J Vasc Surg 1987;6:578-582.
470 Michel J, Jondeau G, Milewicz DM. From genetics to response to injury : vascular
471 smooth muscle cells in aneurysms and dissections of the ascending aorta.
472 Cardiovasc Res 2018;578-589.
473 Miura K. Application of scanning acoustic microscopy to pathological diagnosis. In:
474 Stanciu SG, ed. Microsc Anal Croatia: Intech, 2016. pp. 381-403.

475 Miura K, Egawa Y, Moriki T, Mineta H, Harada H, Baba S, Yamamoto S. Microscopic
476 observation of chemical modification in sections using scanning acoustic
477 microscopy. Pathol Int 2015;65:355-366.
478 Miura K, Katoh H. Structural and histochemical alterations in the aortic valves of
479 elderly patients: A comparative study of aortic stenosis, aortic regurgitation, and
480 normal valves. Biomed Res Int 2016;2016.
481 Miura K, Yamamoto S. A scanning acoustic microscope discriminates cancer cells in
482 fluid. Sci Rep 2015;5.
483 Radu-Ionita F, Ţintoiu IC, Rosu A, Bontas E, Cochior D, Bolohan R, Silvestru C, Ifrim
484 M, Mocanu I, Riga D, Murgu V, Riga S, Savoiu D, Kibos A. Aging aorta-cellular
485 mechanisms. New Approaches to Aortic Dis from Valve to Abdom Bifurc
486 2017;3-23.
487 Saijo Y. Acoustic microscopy: latest developments and applications. Imaging Med
488 London: Future Medicine Ltd 2009;1:47-63.
489 Saijo Y, Sasaki H, Okawai H, Nitta S, Tanaka M. Acoustic properties of atherosclerosis
490 of human aorta obtained with high-frequency ultrasound. Ultrasound Med Biol
491 1998;24:1061-1064.
492 Sasaki H, Saijo Y, Tanaka M, Okawai H, Terasawa Y, Yambe T, Nitta SI. Influence of

tissue preparation on the high-frequency acoustic properties of normal kidney tissue. Ultrasound Med Biol 1996;22:1261-1265.

Schmitt C, Hadj Henni A, Cloutier G. Ultrasound dynamic micro-elastography applied to the viscoelastic characterization of soft tissues and arterial walls. Ultrasound Med Biol 2010;36:1492-1503.

Sottile J. Fibronectin polymerization regulates the composition and stability of extracellular matrix fibrils and cell-matrix adhesions. Mol Biol Cell 2002;13:3546-3559.

Sutton-Tyrrell K, Najjar SS, Boudreau RM, Venkitachalam L, Kupelian V, Simonsick EM, Havlik R, Lakatta EG, Spurgeon H, Kritchevsky S, Pahor M, Bauer D, Newman A. Elevated aortic pulse wave velocity, a marker of arterial stiffness, predicts cardiovascular events in well-functioning older adults. Circulation 2005;111:3384-3390.

Tsamis A, Krawiec JT, Vorp DA. Elastin and collagen fibre microstructure of the human aorta in ageing and disease: a review. J R Soc Interface 2013;10:20121004.

Waddell TK, Dart AM, Gatzka CD, Cameron JD, Kingwell BA. Women exhibit a greater age-related increase in proximal aortic stiffness than men. J Hypertens 2001;19:2205-2212.

511 Weiss EC, Anastasiadis P, Pilarczyk G, Lemor RM, Zinin P V. Mechanical properties
512 of single cells by high-frequency time-resolved acoustic microscopy. IEEE Trans
513 Ultrason Ferroelectr Freq Control 2007;54:2257-2271.
514 Wittek A, Karatolios K, Bihari P, Schmitz-Rixen T, Moosdorf R, Vogt S, Blase C. In
515 vivo determination of elastic properties of the human aorta based on 4D ultrasound
516 data. J Mech Behav Biomed Mater 2013.
517 Wu D, Shen YH, Russell L, Coselli JS, Lemaire SA. Molecular mechanisms of thoracic
518 aortic dissection. J. Surg. Res. 2013.
519
520
521

522 **Figure captions**

523

524 **Fig. 1 Flow chart of SAM observation**

525

526 **Fig. 2** Relationship among age, **mean** speed-of-sound (SOS), and grade of medial
527 degeneration (MDG) in normal and dissected aortae

528 a. Relationship between average SOS value and age of normal and dissection aortae. b.
529 Relationship between MDG scores and age of normal and dissected aortae. **c.**
530 **Relationship between SOS value and MDG scores. d. Boxplot showing the SOS and**
531 **MDG difference between normal and dissected cases.** *r* = Peason's correlation
532 coefficient.

533

534 **Fig. 3** Representative speed-of-sound (SOS) images of the aortae after collagenase
535 type-III digestion (a: 85-year-old woman, b: 31-year-old man, c: Marfan (MF)
536 syndrome, d: Non-MF syndrome)

537 SOS images exhibited gradual decreases in SOS values at 1.5 h and 3 h after digestion.
538 The corresponding light microscopy (LM) images of Elastica Masson trichrome (EMT)
539 staining before and after 3 h of collagenase digestion are shown in the upper rows. The
540 elderly aorta (b) appears with more fragmentation of elastic fibers. The aortae in both

MF (c) and non-MF (d) cases exhibit rapidly decreasing SOS values after collagenase digestion. The MF case with cystic mucoid degeneration shows punctate low SOS areas on the right side. The non-MF aorta consisting of parallel muscle fibers and wavy elastic fibers with focal splitting shows high SOS at the baseline. Black bar = 400 μm, red bar = 10 μm.

Fig. 4 Reduction of SOS after collagenase digestion (left: young and old, right: dissection and age-matched normal controls)

SOS of all groups decreased from 0 to 1.5 h, and 1.5 h to 3 h after collagenase digestion. SOS values in dissection cases decreased more rapidly than those in normal age-matched aortae. ***$p < 0.001$, **$p < 0.01$, *$p < 0.05$.

Fig. 5 Immunostaining with anti-smooth muscle actin (SMA) (a), anti-collagen type-I (COL 1) (b), and anti-collagen type-III (COL 3) (c) antibodies of young, elderly, MF, and non-MF sections

Regarding the SMA, the young aortae showed parallel linear smooth muscles, whereas the old aortae exhibited split smooth muscle fibers. MF cases displayed aggregated SMA bundles with irregular arrangement, whereas non-MF cases showed frayed muscle

559 fibers with irregular arrangement. Regarding COL 1 and COL 3, young and elderly
560 cases displayed parallel fiber components between smooth muscle fibers, although the
561 fiber array was irregular in old cases. MF cases had irregular fiber arrangements among
562 cells, whereas non-MF cases exhibited rich collagen fibers in a focal irregular array.
563
564 **Fig. 6** Immunostaining with anti-lysyl oxidase (LOX) (a), vitronectin (VN) (b), fibrillin
565 (FBN) (c), and fibronectin (FN) (d) antibodies of young, elderly, MF, and non-MF
566 sections
567 The normal young aorta was negative for LOX, whereas the old aorta showed focal
568 faint positivity. MF aortae exhibited strong punctate positivity on smooth muscles for
569 LOX, whereas non-MF aortae showed focal weak positivity. In VN, all normal young or
570 old aortae and MF and non-MF aortae, displayed focal positivity, although MF cases
571 show rather irregular distribution. For FBN, only MF cases exhibited negative. For FN,
572 old and non-MF cases show positivity along muscle fibers.
573

Fig. 1

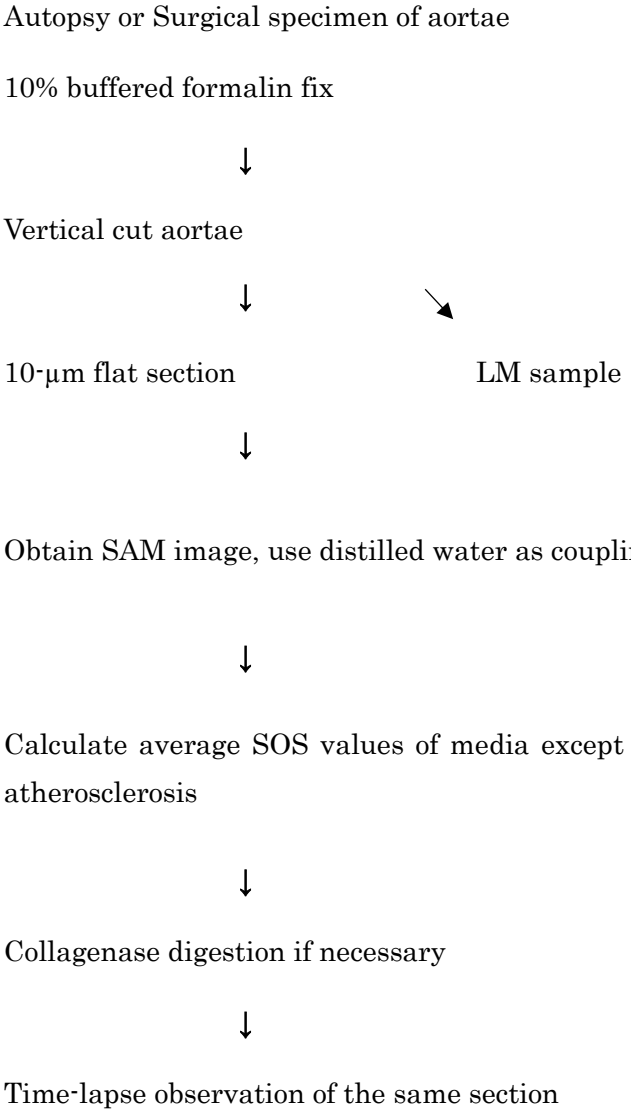
Autopsy or Surgical specimen of aortae
10% buffered formalin fix
Vertical cut aortae
10-μm flat section
LM sample
Obtain SAM image, use distilled water as coupling medium
Calculate average SOS values of media except calcification and severe atherosclerosis
Collagenase digestion if necessary
Time-lapse observation of the same section

Fig. 2a

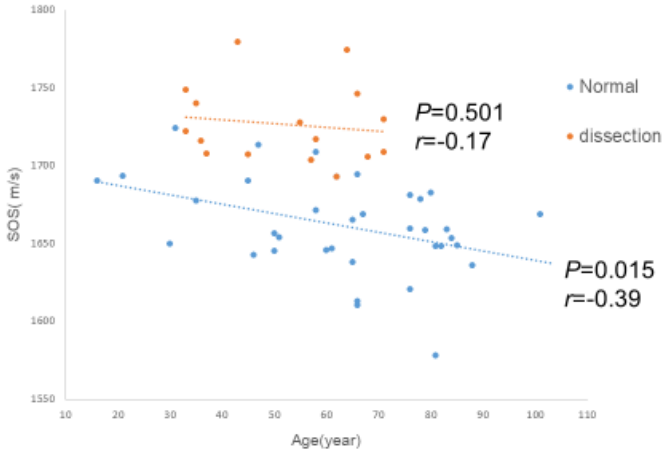
1800
1750
1700
1650
1600
1550
SOS(m/s)
10
20
30
40
50
60
70
80
90
100
110
Age(year)
Normal
dissection
P=0.501
r=-0.17
P=0.015
r=-0.39

Fig. 2b

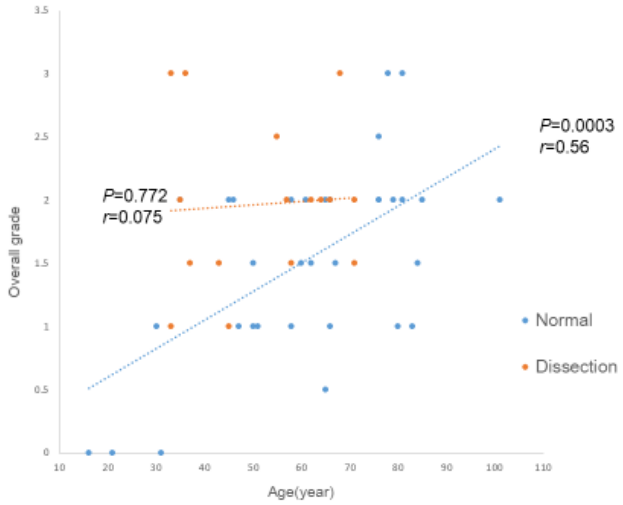
P=0.0003
r=0.56
P=0.772
r=0.075
Normal
Dissection
Overall grade
Age(year)
0
0.5
1
1.5
2
2.5
3
3.5
10
20
30
40
50
60
70
80
90
100
110

Fig. 2c

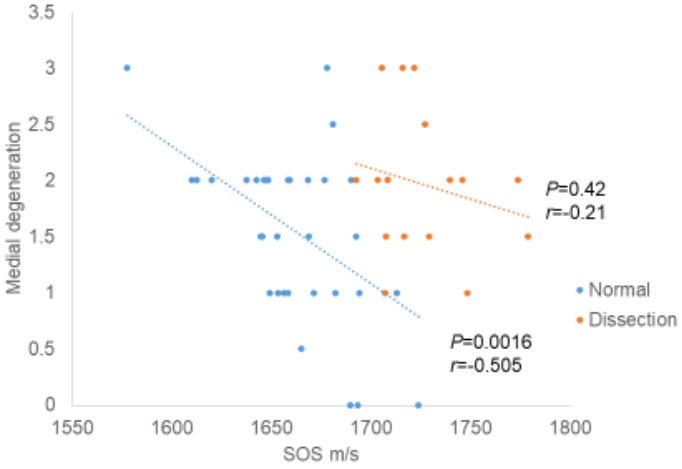
3.5
3
2.5
2
1.5
1
0.5
0
Medial degeneration
1550
1600
1650
1700
1750
1800
SOS m/s
P=0.42
r=-0.21
P=0.0016
r=-0.505
Normal
Dissection

Fig. 2d

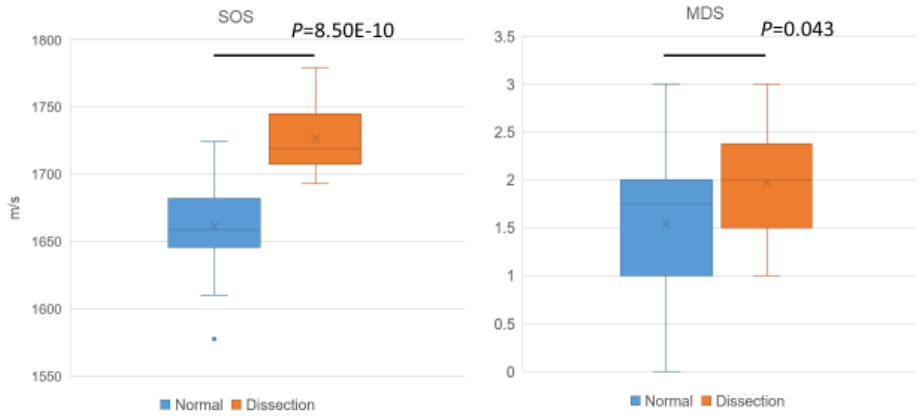
SOS
P=8.50E-10
m/s
1800
1750
1700
1650
1600
1550
Normal
Dissection
MDS
P=0.043
3.5
3
2.5
2
1.5
1
0.5
0
Normal
Dissection

Fig. 3a

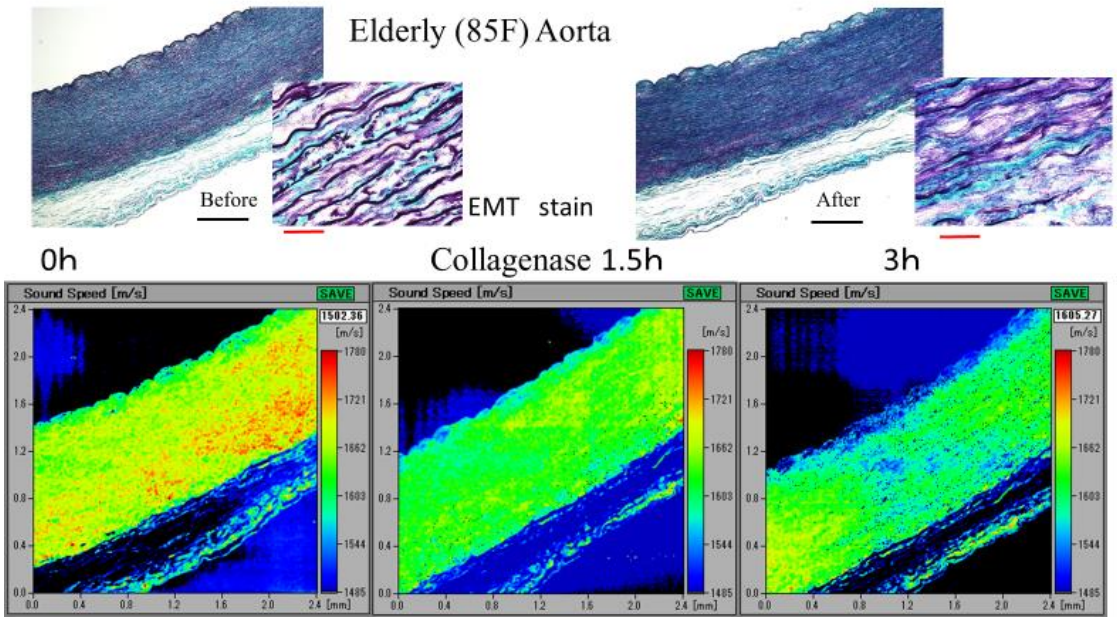
Elderly (85F) Aorta
Before
EMT stain
After
0h
Collagenase 1.5h
3h
Sound Speed [m/s]
SAVE
1502.36
1685.27
[m/s]
1780
1721
1662
1603
1544
1485
[mm]

Fig. 3b

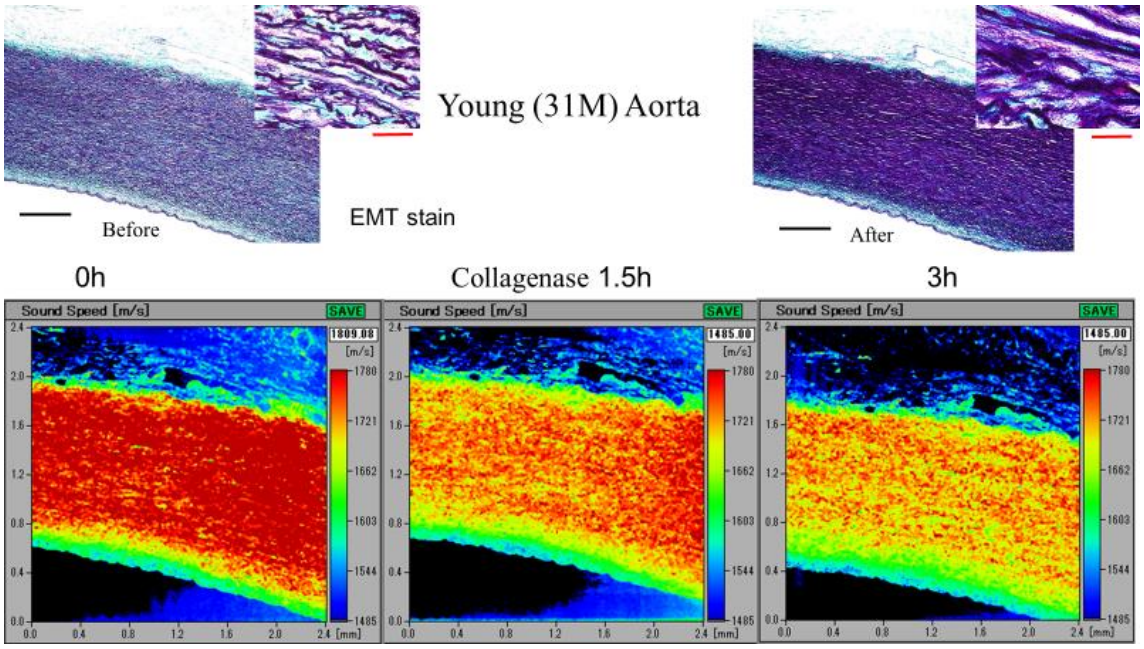
Young (31M) Aorta
Before
EMT stain
After
0h
Collagenase 1.5h
3h
Sound Speed [m/s]
SAVE
1809.08
1485.08
1485.00
[m/s]
1780
1721
1662
1603
1544
1485
[mm]

Fig. 3c

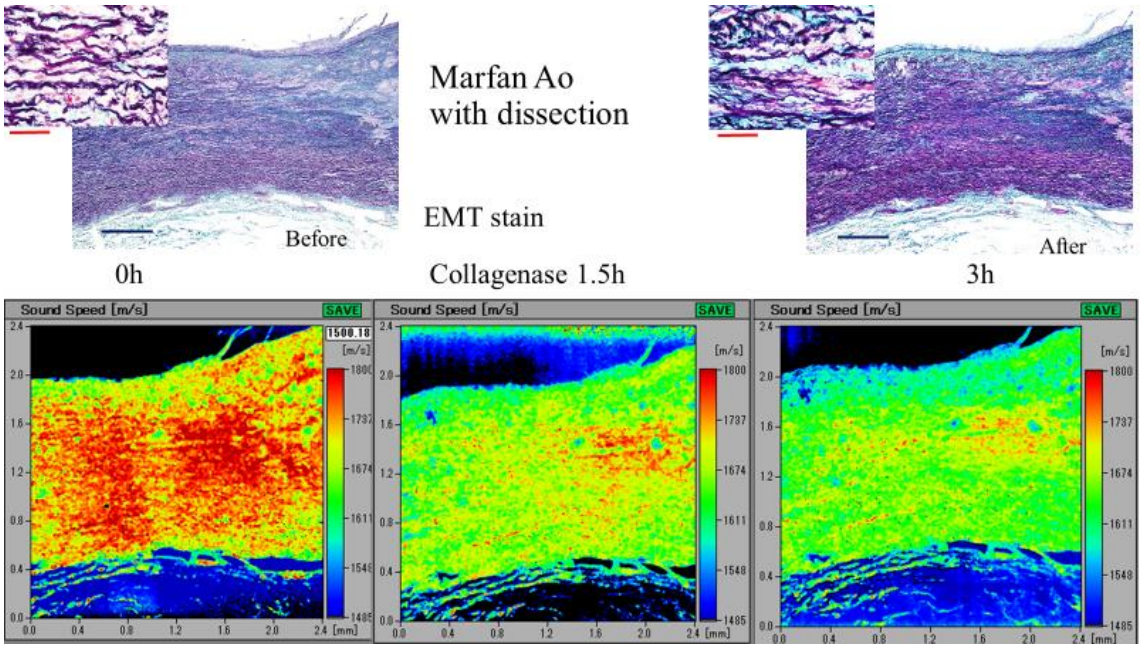
Marfan Ao
with dissection
EMT stain
Before
After
0h
Collagenase 1.5h
3h
Sound Speed [m/s]
SAVE
[m/s]
[mm]

Fig. 3d

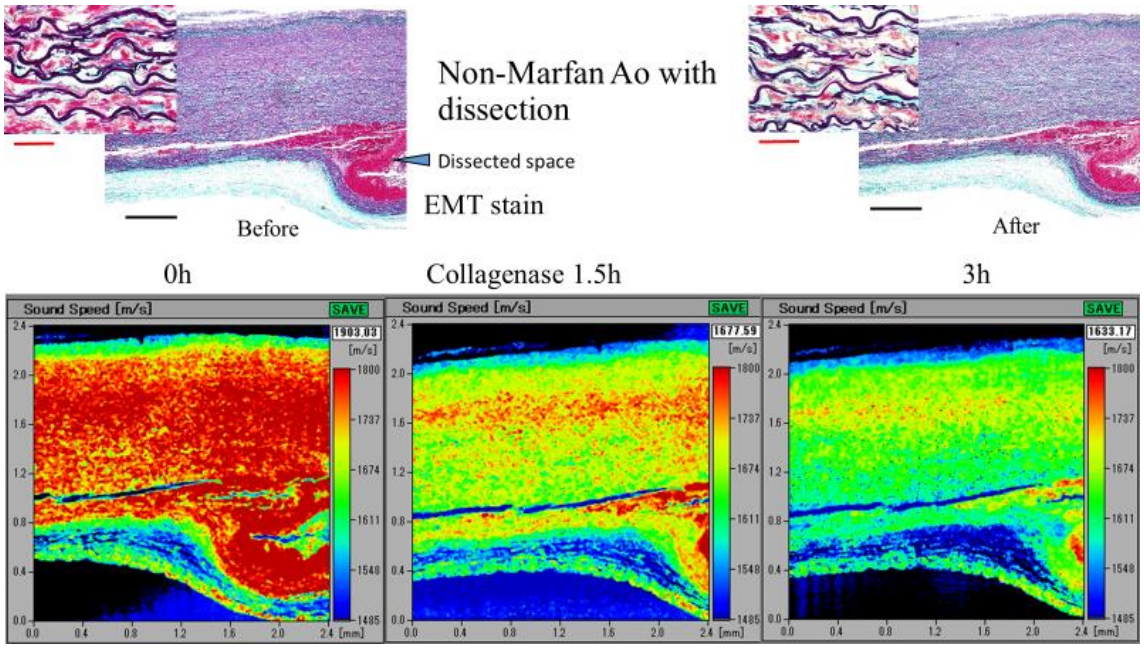
Non-Marfan Ao with dissection
Dissected space
EMT stain
Before
After
0h
Collagenase 1.5h
3h
Sound Speed [m/s]
SAVE
1903.03
1677.59
1633.17
[m/s]
1800
1737
1674
1611
1548
1485
[mm]

Fig. 4

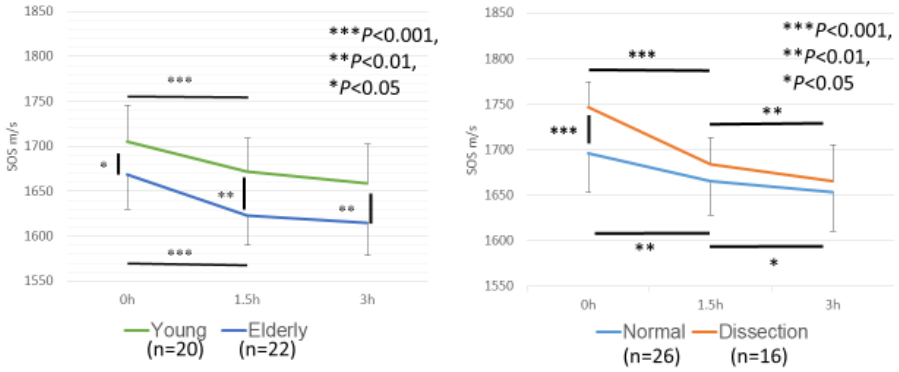
***P<0.001,
**P<0.01,
*P<0.05
SOS m/s
1850
1800
1750
1700
1650
1600
1550
0h
1.5h
3h
Young (n=20)
Elderly (n=22)
Normal (n=26)
Dissection (n=16)

Fig. 5a

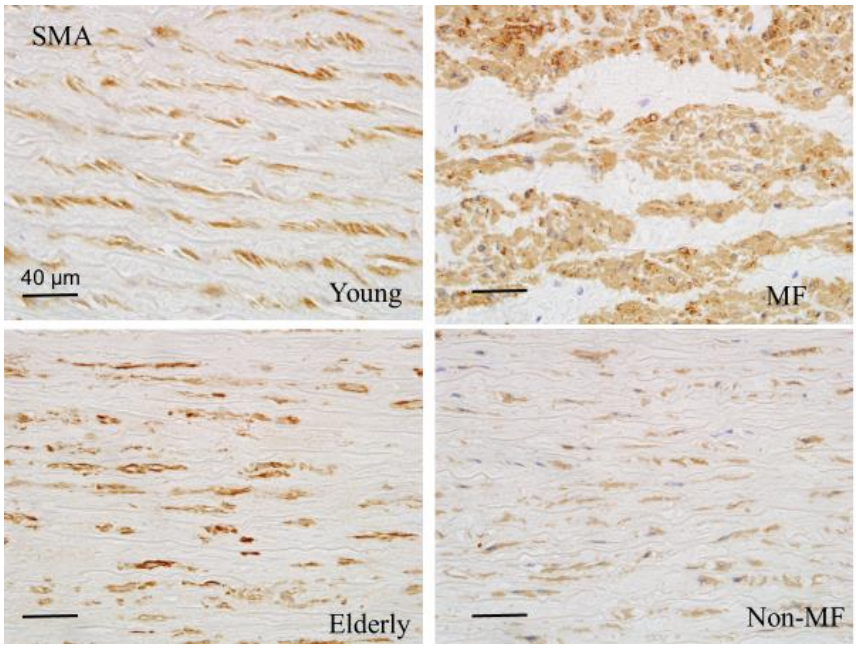

Fig. 5b

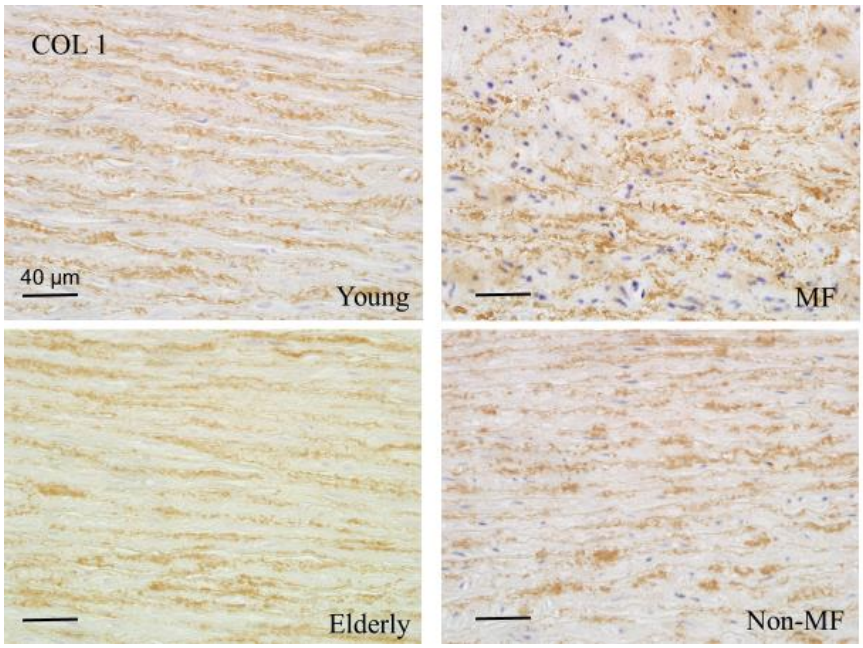

Fig. 5c

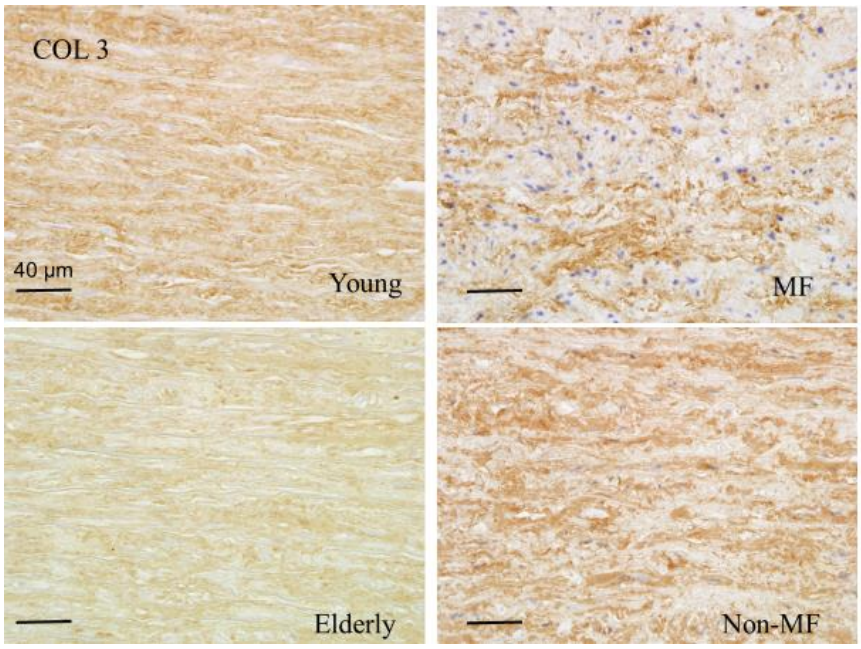

Fig. 6a

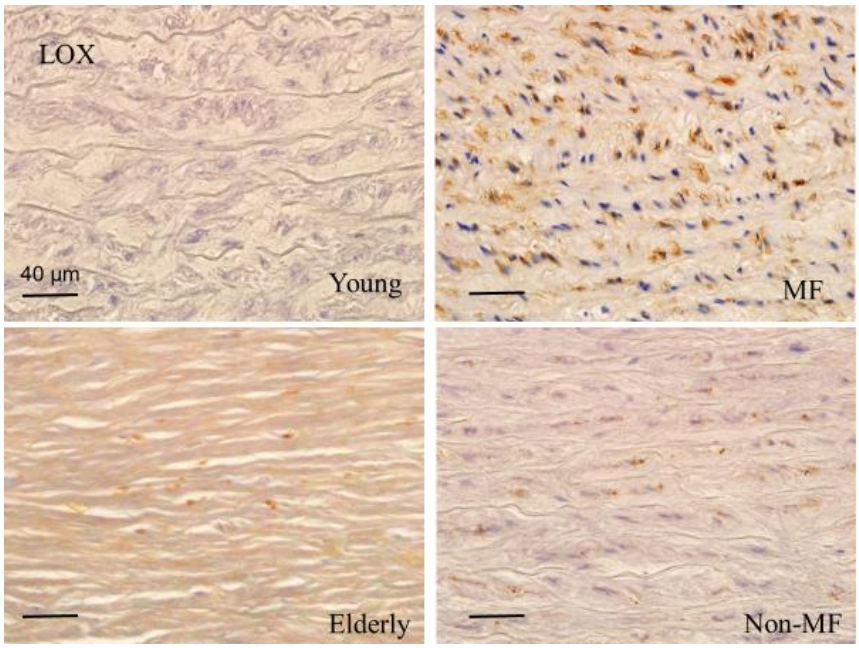

Fig. 6b

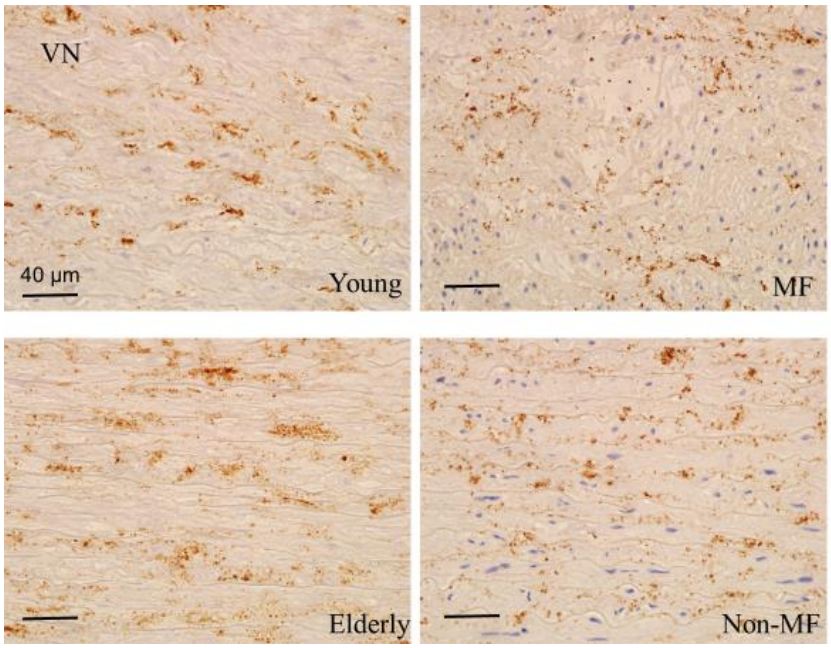

Fig. 6c

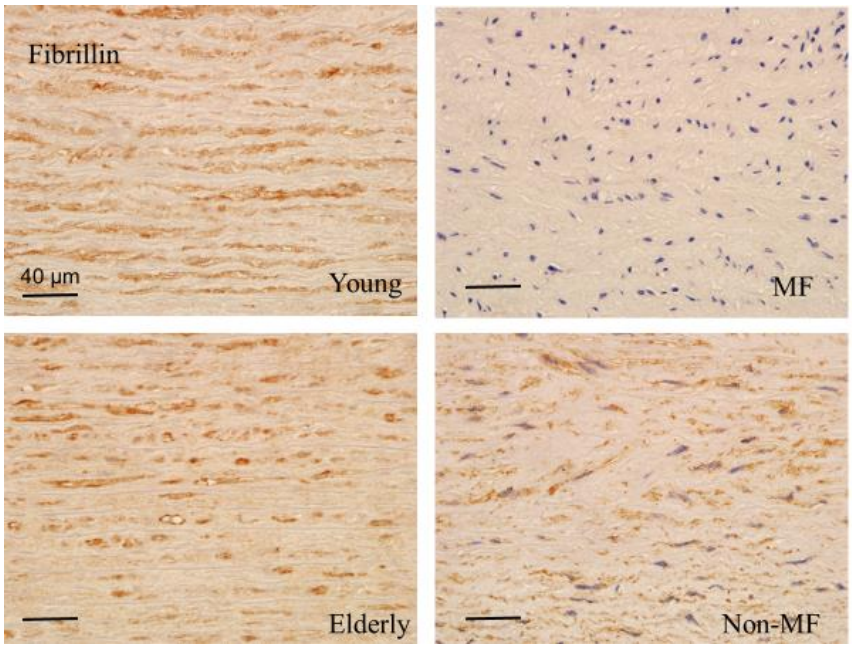

Fig. 6d

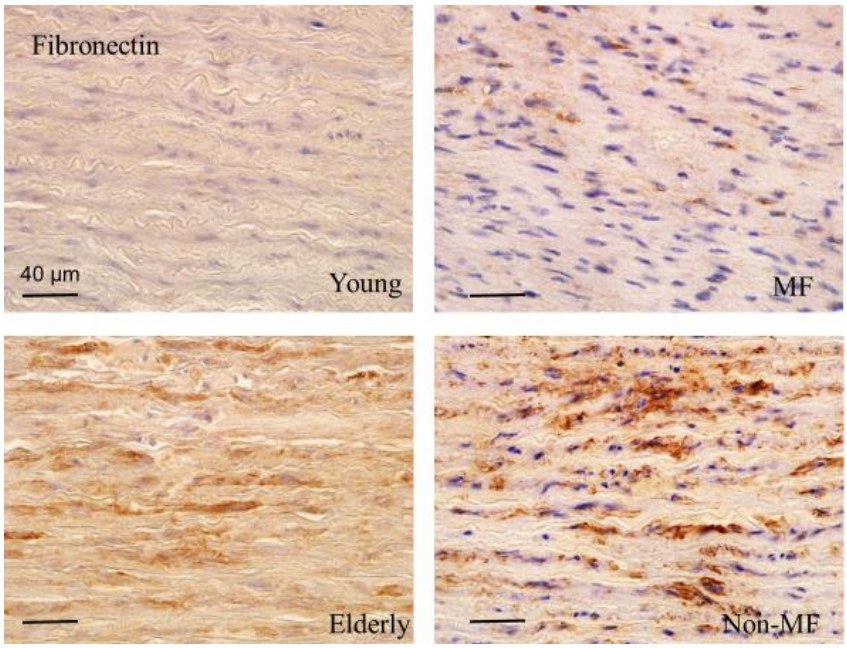

Table

Table 1. Immunostaining results of the supporting components

Case	SMA	Col 1	Col 3	LOX	VN	FBN	FN
N-Young	+	+	+	−	+	+	−
N-Old	+F,W	+F,W	+	+W	+F	+	+
MF	+F	+F	+F	++	+	−	+F,W
Non-MF	+F,W	+F,W	+F,W	+F	+	+	+

N-Young, normal young; N-Old, normal old; MF, Marfan syndrome; F, focal; W, weak; SMA, smooth muscle actin; Col 1, collagen type-I; Col 3, collagen type-III; LOX, lysyl oxidase; VN, vitronectin; FBN, fibrillin; FN, fibronectin

Table A.1. Average speed-of-sound (SOS) of older (OL) and younger (YG) aortae after collagenase digestion

Collagenase	**n**	**Average**	**SD**
		m/s	
YG0h	20	1705.1	40.6
YG1.5h	20	1672.3	36.7
YG3h	20	1658.8	43.5
OL0h	22	1668.4	38.1
OL1.5h	22	1622.7	32.9
OL3h	22	1614.5	36.0

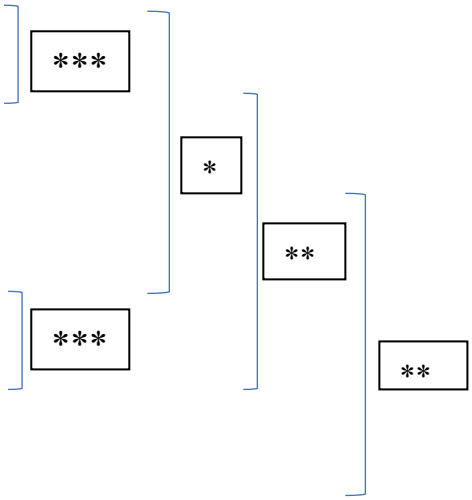

*** $p < 0.001$. ** $p < 0.01$, * $p < 0.05$

Table A.2. Average speed-of-sound (SOS) of normal (NOR) and dissection (DIS) aortae after collagenase digestion.

Collagenase	n	Average m/s	SD	
0h-NOR	26	1695.8	42.5	**
1.5h-NOR	26	1665.6	37.7	*
3h-NOR	26	1653.3	42.5	***
0h-DIS	16	1741.1	27.6	***
1.5h-DIS	16	1684.0	29.0	***
3h-DIS	16	1665.8	39.3	

*** $p < 0.001$, ** $p < 0.01$, * $p < 0.05$